The College of Engineering
University of Wisconsin-Madison

Wisconsin Electric Machines and Power Electronics Consortium

RESEARCH REPORT
92-1

Transient Analysis of Induction Machines Under Internal Faults Using Winding Functions

Y. Liao and T. A. Lipo
Dept. of Electrical and Computer Engineering
University of Wisconsin-Madison
1415 Johnson Drive
Madison, WI 53706

H.A. Toliyat, M.M. Rahimian
Dept. of Electrical Engg.
Ferdowsi University-Mashhad
Mashhad, Iran

WEMPEC

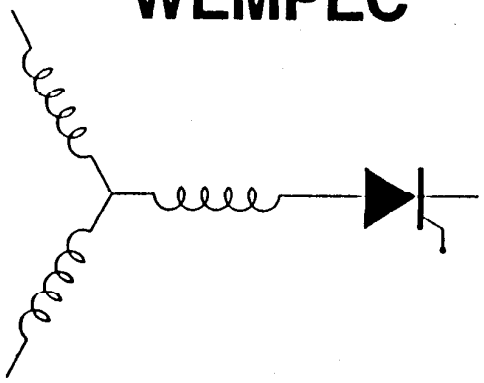

Department of Electrical and Computer Engineering
1415 Johnson Drive
Madison, Wisconsin 53706

TRANSIENT ANALYSIS OF INDUCTION MACHINES UNDER INTERNAL FAULTS USING WINDING FUNCTIONS

H.A. Toliyat* S. Bhattacharya† M.M. Rahimian* T.A. Lipo†
†Dept. of Electrical & Computer Engg., University of Wisconsin
1415 Johnson Drive, Madison, WI 53706 USA
Tel: 608-262-5559 Fax: 608-262-1267

*Dept. of Electrical Engg., Ferdowsi University-Mashhad,
Mashhad, Iran

ABSTRACT

This paper proposes the use of a "Winding Function Approach to Induction Machine Modelling", of the transient analysis of the induction machine operating under asymmetrical conditions of stator and/or rotor winding connections. This approach, based on the winding functions, makes no assumption as to the necessity for sinusoidal MMF and hence accounts for all the space harmonics in the machine. In this paper, modelling of the effects of asymmetry in the stator, arising due to an interturn fault resulting in a disconnection of one or more coils making up a portion of a stator phase winding; and the effects due to asymmetry in the rotor, arising because of broken rotor bars are examined. Simulation and experimental results confirm the validity of the proposed approach.

1.0 INTRODUCTION

The induction machine can operate under asymmetrical stator and/or rotor winding connections during such conditions as:

* Abnormal connection of the stator windings;
* Insertion of line impedance in one phase to obtain specific torque-speed characteristics for the purpose of starting or braking;
* Insertion of single phase auto transformers of unequal impedances;
* Asymmetrical disposition in space of the magnetic axes of the stator phase windings;
* A difference in the effective number of turns of the stator phase windings;
* A difference in the conductor sizes of the stator phase windings;
* A difference in the spread of the coil groups per pole of the stator phase windings;
* A difference in the placement of the coils in the stator slots;
* Interturn fault resulting in the opening or shorting of one or more circuits of a stator phase winding;
* Broken rotor bar or broken end-ring;

Asymmetrical operation of the induction machine under any of the above conditions results in unbalanced air gap voltages. This leads to large unbalanced line currents, increased losses in the machine, increased torque pulsations, decreased average torque and increased slip of the machine. Consequently, asymmetrical operation of the induction machine results in poor efficiency and excessive heating, which eventually leads to the failure of the machine. Since this mode of operation is typically undesirable, characterization and accurate prediction of the degradation of the performance of the induction machine under such conditions is of considerable importance, since it results in shortened operating life and derating of the machine. Also, determination of adequate protective equipment for large unbalanced line currents due to asymmetrical operation is of importance. This is due to the fact that the small unbalances in the voltages due to the asymmetrical stator and/or rotor winding connections may cause larger unbalances in the line currents, and it is difficult to provide adequate protective equipment for the motor when the line currents are greatly unbalanced. The transient analysis of the induction machine with asymmetrical stator and/or rotor winding connections, is important also, for on-line monitoring of large motors.

Traditionally, the phasor symmetrical component theory [1-3] has been used for the steady state analysis of induction machines with asymmetrical stator winding connections operating with balanced or unbalanced sinusoidal voltage supply. However, this method lacks the

ability to predict the transient characteristics of the machine. Instantaneous symmetrical component theory has been proposed [4-5], for the transient analysis of the induction machine with asymmetrical connections in the stator windings only, to predict the transient characteristics but must typically involve only a single space harmonic. The generalized rotating field theory [6-12] has also been used to derive the equivalent d-q-o models for the induction machines operating with asymmetrical stator winding connections. The derivation of the equivalent d-q-o models from the generalized rotating field theory is based on the assumption of sinusoidal MMF in the machine. The d-q-o models based on the generalized rotating field theory, and the instantaneous symmetrical component theory based models, have also been used for the transient analysis of the induction motor with series SCR controlled voltage supply [13-14]. Thus, both the equivalent d-q-o model based approach and the instantaneous symmetrical component based approach, disregard any existence of the space harmonics in the machine.

The existence of space harmonics is well known to have a significant detrimental effect on the steady state and transient characteristics of the machine, such as overheating and significant torque pulsations which may cause cogging and crawling. Thus, the existing approaches lack the ability to predict the derating of the machine required due to the adverse effects of the space harmonics, either with balanced sinusoidal voltage supply, series SCR controlled voltage supply or various types of inverter supply.

The transient analysis of the induction machine for the case of the rotor asymmetry, resulting due to either a broken rotor bar or broken end-ring, has in general received less attention than the case of stator asymmetry. Weichel and Mishkin [15-16], discuss the case of rotor asymmetry arising due to the broken end-ring for a squirrel-cage induction machine. Steady-state analysis of the induction machine for the case of rotor asymmetry, due to broken rotor bars has already been reported in [17-19], based on the method of symmetrical component theory and in [20], using d-q-o theory. As already mentioned, this analysis is based on the assumption of the absence of higher order space harmonics in the machine and cannot accurately predict the transient characteristics of the machine. Thus, tools for the transient analysis of the induction machine for the case of rotor asymmetry, due to a broken rotor bar and/or end-ring are not available. A computer based instrument for detection of broken rotor bars and open end-rings in squirrel cage induction motors has been reported in [21]. The adverse effects of broken rotor bars in squirrel cage induction motors are excessive vibration, noise and sparking during starting. These effects become noticeable when the fault in the rotor has substantially grown to involve several broken bars, making the detection of one broken rotor bar in the machine, as mentioned in [21] a very difficult task.

This paper proposes the use of a winding function approach to induction machine modelling of the transient analysis of the induction machine with asymmetrical stator and/or rotor winding connections in Section 2 [21,23]. This approach, makes no assumption as to the necessity for sinusoidal MMF and hence accounts for all the space harmonics in the machine. This approach has been applied previously to predict the performance of induction and synchronous reluctance machines [24,25], with multiple phases and general winding connections such as concentrated, concentric and multiple layer with different pitch factor, including space and time harmonics. This problem of effectively modelling the asymmetries in the stator and rotor with the concomitant effects of space harmonics is of increasing importance for studying the degradation of the performance of induction motor drive systems and for on-line monitoring of large motors.

With the proliferation of inverter supplied induction motors for adjustable speed drives (ASDs) systems, characterization and accurate prediction of the degradation of the transient performance of the motor drive system arising due to the asymmetrical stator and/or rotor winding connections, has become of paramount importance. This is because of the necessity of accurate determination of the additional derating required of the motor, due to the adverse effects of non-sinusoidal impressed voltages.

Section 3 gives the simulation results for asymmetrical stator winding connection, due to a disconnection of one of the two coils making up a stator phase, and for rotor asymmetry arising due to a broken rotor bar, with balanced sinusoidal voltage supply and six step voltage source inverter supply.

Section 4 gives the steady state experimental results for the case of asymmetrical stator winding connections with balanced sinusoidal voltage supply.

In all cases of asymmetrical operation of the induction motor it is imperative to estimate the effective stress imposed on the motor and to ensure that the operating condition is well within the rating of the motor. This paper thus attempts to provide a generalized method for the transient analysis of the induction machine with asymmetrical stator and/or rotor winding connections. Section 5 enumerates the important conclusions of the proposed approach.

2.0 MUTUALLY COUPLED MAGNETIC CIRCUIT APPROACH USING WINDING FUNCTIONS.

Accurate calculation of the machine apparent and incremental inductances and their variation with the rotor angle is crucial for the transient analysis of the machine. This is especially true for the case of induction machine with asymmetrical stator and/or rotor winding connections, with either balanced sinusoidal voltage supply or with various types of inverter supply. Induction machines with asymmetrical stator and/or rotor winding connections, supplied with balanced sinusoidal voltages, result in unbalanced currents and MMF waveforms with space harmonics. An accurate prediction of the transient analysis of the machine cannot be achieved by the uniformly rotating d-q-o frame of reference due to the non-sinusoidal MMF waveforms so generated in the air-gap.

The problem of accurate prediction of the transient analysis of the induction machine is more acute with various types of inverter supply, which are characterized by either non-sinusoidal voltage (Voltage Source Inverters - VSI) or current (Current Source Inverters - CSI) waveforms, and which consequently induce non-sinusoidal MMF waveforms. This problem becomes more serious for induction machines with asymmetrical stator and/or rotor winding connections and supplied by inverters. In such cases the MMF waveforms are again non-sinusoidal and in addition the MMF waveform jumps in discrete steps. Also, the rate of change of the currents (di/dt), is much higher than those encountered in the case of balanced sinusoidal voltage supply, due to inverter switching. Hence, for accurate prediction of the transient behavior of the machine under such conditions, accurate values of the self and mutual incremental machine winding inductances ($d\lambda/di$) are required, rather than their apparent values (λ/i). This is because the inductive voltage terms ($d\lambda/dt$), encountered in the machine models can be expressed as $[(d\lambda/di) . (di/dt)]$.

Asymmetrical operation of the induction machine due to the asymmetrical stator and/or rotor winding connection results in a non-sinusoidally distributed winding as opposed to the conventional distributed winding of the machine. Loss of one of the two coils making up one phase of the stator, for example, would clearly result in concentrated or non-sinusoidally distributed winding on the stator. In this case, the entire phase belt is located in one slot, or the windings are concentrated with unity pitch and distribution factor. Similarly, a broken rotor bar would also result in higher harmonic MMFs in the rotor. Hence, a new mutually coupled magnetic circuit model is derived for the concentrated winding machines based on the winding function approach [22]. Equations which define the transient as well as steady state behavior including the computation of all machine inductances are derived. Equations for calculation of electromagnetic torque have also been modified to account for non sinusoidal air gap flux distributions.

2.1 Modelling of Induction Machines with Non-sinusoidally Distributed Windings

As mentioned previously, the d-q-o model of induction machines is based on the assumption that only the fundamental and no higher order harmonics exist, due to the stator winding distribution. While a valid approximation for conventional distributed winding machines; however, replacement of concentrated windings (square wave windings) with equivalent sinusoidal windings, is clearly not valid if reasonable approximations of the machine voltage and current wave shapes are to be obtained. Hence the analysis of the machine under such conditions becomes complicated due to the fact that the usual transformations no longer yield a simplification in the model. In this study, we are particularly interested in the effects of these space harmonics in the MMF waveforms. The coupled magnetic circuit approach is used to derive a new mathematical model of a general concentrated winding machine with m phase stator windings, n rotor bars (m-n winding machine). The machine is simulated in the so-called natural frame of reference. That is, the machine is simulated in terms of the actual physical variables, rather than transformed or equivalent variables. The model is applicable to both squirrel cage and phase wound rotors and also for cage

rotors with non-integral numbers of rotor bars per stator pole-pair.

2.2 Equations for an m-n Concentrated Winding Machine

Consider initially a general m-n winding machine with the following assumptions,

- negligible saturation
- uniform air-gap
- m identical stator windings with axes of symmetry
- n uniformly distributed cage bars or identical rotor windings with axes of symmetry such that even harmonics of the resulting spatial winding distribution are zero
- eddy current, friction, and windage losses are neglected

The cage rotor can be viewed as n identical and equally spaced rotor loops. For example, the first loop may consist of the 1st and (k+1)th rotor bars and the connecting portions of the end rings between them, where k is any arbitrarily chosen integer ($1 \le k \le n$) and the second loop consists of the 2nd and (k+2)th rotor bar and the connecting portions of the end rings between them and so on.

2.3 Stator Voltage Equations

The voltage equations for the stator loops can be written as,

$$V_s = R_s I_s + \frac{d\Lambda_s}{dt} \tag{1}$$

where,

$$\Lambda_s = L_{ss} I_s + L_{sr} I_r \tag{2}$$

and

$$I_s = \left(i_1^s \; i_2^s \ldots\ldots\ldots\ldots i_m^s\right) t \tag{3}$$

$$I_r = \left(i_1^r \; i_2^r \ldots\ldots i_n^r\right) t \tag{4}$$

$$V_s = \left(v_1^s \; v_2^s \ldots\ldots\ldots\ldots v_m^s\right) t \tag{5}$$

The matrix R_S is a diagonal m x m matrix given by,

$$R_s = r_s I \tag{6}$$

where, I is an m x m identity matrix and r_S is the resistance of each coil assuming all coils are similar. Due to conservation of energy, the matrix L_{ss} is a symmetric m x m matrix of the form,

$$L_{ss} = \begin{pmatrix} L_{11}^s & L_{12}^s & \ldots\ldots\ldots\ldots & L_{1m}^s \\ L_{21}^s & L_{22}^s & \ldots\ldots\ldots\ldots & L_{2m}^s \\ \vdots & \vdots & & \vdots \\ \vdots & \vdots & \ldots\ldots\ldots\ldots & \vdots \\ L_{m1}^s & L_{m2}^s & \ldots\ldots\ldots\ldots & L_{mm}^s \end{pmatrix} \tag{7}$$

The mutual inductance matrix L_{sr} is a m x n matrix comprised of the mutual inductances between the stator coils and the rotor loops.

$$L_{sr} = \begin{pmatrix} L_{11}^{sr} & L_{12}^{sr} & \ldots\ldots\ldots\ldots & L_{1n}^{sr} \\ L_{21}^{sr} & L_{22}^{sr} & \ldots\ldots\ldots\ldots & L_{2n}^{sr} \\ \vdots & \vdots & & \vdots \\ \vdots & \vdots & \ldots\ldots\ldots\ldots & \vdots \\ L_{m1}^{sr} & L_{m2}^{sr} & \ldots\ldots\ldots\ldots & L_{mn}^{sr} \end{pmatrix} \tag{8}$$

Since the inductance matrix L_{ss} is constant, whereas L_{sr} varies with the position of the rotor, the second term of Eq. (1) can be written as,

$$\frac{d\Lambda_s}{dt} = L_{ss}\frac{dI_s}{dt} + \frac{dL_{sr}}{dt} I_r + L_{sr}\frac{dI_r}{dt} \tag{9}$$

Further, the second term in the above equation (9), can be written using the chain rule as,

$$\frac{dL_{sr}}{dt} I_r = \frac{dL_{sr}}{d\theta_{rm}} \frac{d\theta_{rm}}{dt} I_r \tag{10}$$

where, θ_{rm} is the spatial position of the rotor.
Defining rotor mechanical speed as,

$$\omega_{rm} = \frac{d\theta_{rm}}{dt} \tag{11}$$

then,

$$\frac{dL_{sr}}{dt} I_r - \omega_{rm} \frac{dL_{sr}}{d\theta_{rm}} I_r \tag{12}$$

Therefore, Eq. (9) can typically be written in the form,

$$\frac{d\Lambda_s}{dt} = L_{ss}\frac{dI_s}{dt} + \omega_{rm}\frac{dL_{sr}}{d\theta_{rm}} I_r + L_{sr}\frac{dI_r}{dt} \tag{13}$$

2.4 Rotor Voltage Equations

The representation of an induction machine with a cage rotor is fundamentally the same as one with a phase wound rotor where it is assumed that the cage rotor can be replaced by a set of mutually coupled loops.One particular advantage of this approach is that it is also applicable to cage rotors with non-integral numbers of rotor bars per pole-pair.

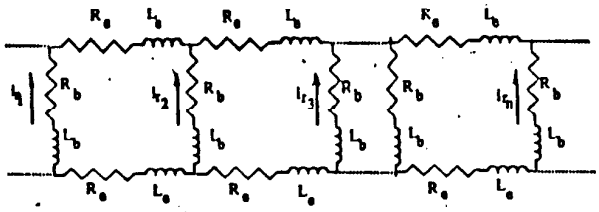

Figure 1 Equivalent circuit of squirrel cage rotor.

From Fig. 1 the voltage equations for the rotor loops are,

$$V_r = R_r I_r + \frac{d\Lambda_r}{dt} \qquad (14)$$

where,

$$V_r = \left(v_1^r\ v_2^r \ldots\ldots\ldots\ldots v_n^r\right)^t$$

In case of a cage rotor $v_k^r = 0$: k=1.2.....n. The matrix R_r is n x n, symmetric and cyclic. The rows after the first can therefore be obtained by circular permutation. Each succeeding row is obtained from the previous row one step to the right with the last element inserted in the first column or,

$$R_r = \begin{pmatrix} 2(R_b+R_e) & -R_b & 0 & \ldots\ldots & -R_b \\ -R_b & 2(R_b+R_e) & -R_b & \ldots\ldots & 0 \\ \vdots & \vdots & \vdots & \ldots\ldots & \vdots \\ 0 & 0 & \ldots\ldots & 2(R_b+R_e) & -R_b \\ -R_b & 0 & \ldots\ldots & -R_b & 2(R_b+R_e) \end{pmatrix} \qquad (15)$$

where, R_e is the end ring resistance, and R_b is the rotor bar resistance. The rotor flux linkages Λ_r can be written as,

$$\Lambda_r = L_{sr}^t I_s + L_{rr} I_r \qquad (16)$$

where the matrix L_{sr}^t is the transpose of the matrix L_{sr}

and the matrix L_{rr} is the n x n symmetric matrix,

$$L_{rr} = \begin{pmatrix} L_{mr}+2(L_b+L_e) & L_{r_1r_2}-L_b & L_{r_1r_3} & \ldots\ldots & L_{r_1r_n}-L_b \\ L_{r_2r_1}-L_b & L_{mr}+2(L_b+L_e) & L_{r_2r_3}-L_b & \ldots\ldots & L_{r_2r_n} \\ L_{r_3r_1} & L_{r_3r_2}-L_b & L_{mr}+2(L_b+L_e) & \ldots\ldots & L_{r_3r_n} \\ \vdots & \vdots & \vdots & \ldots\ldots & \vdots \\ L_{r_nr_1}-L_b & L_{r_nr_2} & L_{r_nr_3} & \ldots\ldots & L_{mr}+2(L_b+L_e) \end{pmatrix} \qquad (17)$$

In Eq. (17), L_{mr} is the magnetization inductance of each rotor loop, L_b the rotor bar leakage inductance, L_e the rotor end ring leakage inductance, and $L_{r_i r_k}$ the mutual inductance between two rotor loops.

2.5 Calculation of Torque

The mechanical equation of motion depends upon the characteristics of the load which may differ widely from one application to the next . We will assume here, for simplicity, that the torque which opposes that produced by the machine consists only of an inertial torque and an external load torque which are known explicitly. In this case the mechanical equation of motion is simply,

$$J\frac{d^2\theta_{rm}}{dt^2} + T_L = T_e \qquad (18)$$

where θ_{rm} is the angular displacement of the rotor, T_L is the load torque, and T_e is the electromagnetic torque produced by the machine.

The electrical torque can be found from the magnetic coenergy W_{co} as,

$$T_e = \left(\frac{\partial W_{co}}{\partial \theta_{rm}}\right)(I_s, I_r \text{ constant}) \qquad (19)$$

In a linear magnetic system the coenergy is equal to the stored magnetic energy so that,

$$W_{co} = \frac{1}{2}\left(I_s^t\ I_r^t\right)\begin{pmatrix} L_{ss} & L_{sr} \\ L_{sr}^t & L_{rr} \end{pmatrix}\begin{pmatrix} I_s \\ I_r \end{pmatrix} \qquad (20)$$

or,

$$W_{co} = \frac{1}{2} I_s^t L_{ss} I_s + \frac{1}{2} I_s^t L_{sr} I_r + \frac{1}{2} I_r^t L_{sr}^t I_s + \frac{1}{2} I_r^t L_{rr} I_r \quad (21)$$

It is obvious that L_{ss} and L_{rr} contain only constant elements, so that Eq. (19) reduces to

$$T_e = \frac{1}{2} I_s^t \frac{\partial L_{sr}}{\partial \theta_{rm}} I_r + \frac{1}{2} I_r^t \frac{\partial L_{sr}^t}{\partial \theta_{rm}} I_s \quad (22)$$

Since T_e is a scalar, each of the two terms comprising T_e must be a scalar. Because the transpose of a scalar is clearly the scalar itself, it must be true that the second term must equal its transpose, or

$$I_r^t \frac{\partial L_{sr}^t}{\partial \theta_{rm}} I_s = \left(I_r^t \frac{\partial L_{sr}^t}{\partial \theta_{rm}} I_s \right)^t \quad (23)$$

From matrix algebra,

$$\left(A^t B^t C \right)^t = C^t B A$$

so that,

$$I_r^t \frac{\partial L_{sr}^t}{\partial \theta_{rm}} I_s = I_s^t \frac{\partial L_{sr}}{\partial \theta_{rm}} I_r \quad (24)$$

Hence the first term of Eq. (22) is equal to the second. The torque equation reduces to the final form

$$T_e = I_s^t \frac{\partial L_{sr}}{\partial \theta_{rm}} I_r \quad (25)$$

Thus far, it has been assumed, for simplicity, that the machine has only two poles. In general, let P denote the number of motor poles. It is clear that any inductance which is a function of angular displacement undergoes P/2 complete cycles as θ_{rm} varies from 0 to 2π. Hence,

$$\theta_r = \frac{P}{2} \theta_{rm} \quad (26)$$

where, θ_r is the rotor displacement in electrical radians. In terms of θ_r, the torque is given as,

$$T_e = \frac{P}{2} I_s^t \frac{\partial L_{sr}}{\partial \theta_r} I_r \quad (27)$$

Thus, Eq. (18) in terms of θ_r is given as,

$$\frac{2}{P} J \frac{d^2 \theta_r}{dt^2} + T_L = T_e \quad (28)$$

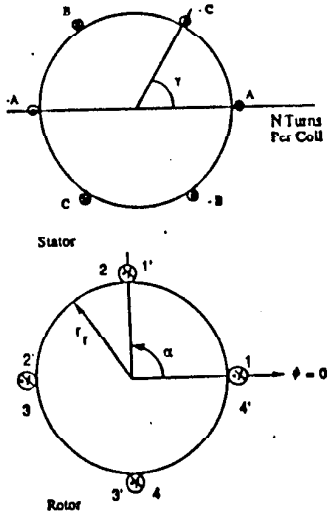

Figure 2 The 3-phase, 2-pole induction machine having two rotor bars per pole.

2.6 Calculation of Inductances of a Concentrated Winding Induction Machine

All of the relevant inductances for the concentrated winding induction machine can be calculated using the winding function method given in [22]. For purposes of illustration the technique is best described by considering an elementary 3 phase, 2 pole induction machine having only 2 rotor bars per pole given in Fig. 2. The winding function for each stator coil is shown in Fig. 3(a) and the winding function for each rotor loop is shown in Fig. 3(b).

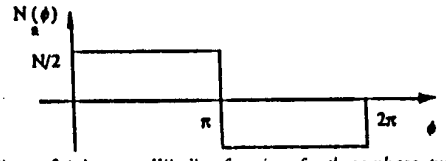

Figure 3-(a) Winding functions for three-phase, two-pole concentrated winding induction motor.

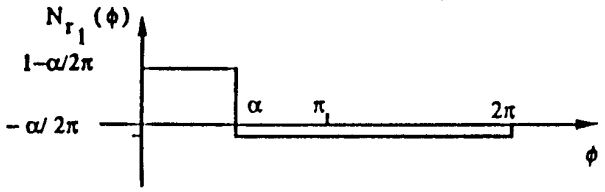

Figure 3-(b) Winding functions for each rotor loop of Figure 2

The magnetizing inductance for each stator coil is given by,

$$L_{ma} = L_{mb} = L_{mc} = \frac{\mu_0 rL}{g} \frac{\pi N^2}{2} \qquad (29)$$

where, r is the average value of the stator inner and rotor outer radius, g is the air-gap, and L is the length of the coil.

Assume γ is the angle between two stator slots in radians which is $\pi/3$ in this case. The mutual inductances between stator phases are

$$L_{ab} = L_{ba} = \frac{\mu_0 rL}{g} \frac{\pi N^2}{2} \left(1 - \frac{4\gamma}{\pi}\right) \qquad (30)$$

$$L_{bc} = L_{cb} = \frac{\mu_0 rL}{g} \frac{\pi N^2}{2} \left(-1 + \frac{2\gamma}{\pi}\right) \qquad (31)$$

$$L_{ac} = L_{ca} = \frac{\mu_0 rL}{g} \frac{\pi N^2}{2} \left(-1 + \frac{2\gamma}{\pi}\right) \qquad (32)$$

where if $\gamma=\pi/3$,

$$L_{ab} = L_{ba} = L_{bc} = L_{cb} = L_{ac} = L_{ca} \qquad (33)$$

Equation (37) expresses the result of assuming that all phases are placed equidistant with respect to each other.

Assume now that α is the angle between two rotor bars in radians. In Fig. 2, α is equal to $\pi/2$. The magnetizing inductance of the rotor loop is given by,

$$L_{mr} = \frac{\mu_0 rL}{g} \alpha \left(1 - \frac{\alpha}{2\pi}\right) \qquad (34)$$

The mutual inductance between any two rotor loops is,

$$L_{r_i r_k} = \frac{\mu_0 rL}{g} \left(-\frac{\alpha^2}{2\pi}\right) \qquad (35)$$

Finally the mutual inductance between stator phase A and rotor loop 1 is as shown in Fig. 4 and given by,

$$L_{ar_1} = \frac{\mu_0 rL}{g} \frac{N}{2} \alpha \qquad 0 \le \theta_{rm} < \pi - \alpha$$

$$L_{ar_1} = \frac{\mu_0 rL}{g} \frac{N}{2} \left(2\pi - 2\theta_{rm} - \alpha\right) \qquad \pi - \alpha \le \theta_{rm} < \pi$$

$$L_{ar_1} = -\frac{\mu_0 rL}{g} \frac{N}{2} \alpha \qquad \pi \le \theta_{rm} < 2\pi - \alpha$$

$$L_{ar_1} = \frac{\mu_0 rL}{g} \frac{N}{2} \left(4\pi - 2\theta_{rm} - \alpha\right) \qquad 2\pi - \alpha \le \theta_{rm} < 2\pi \qquad (36)$$

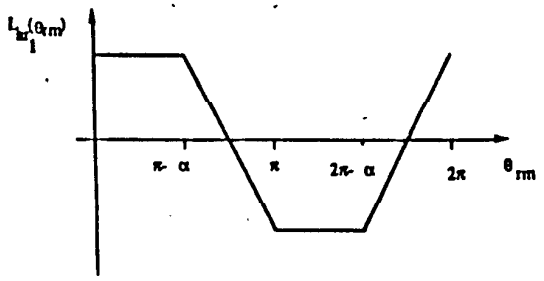

Figure 4 *The mutual inductance between stator phase a and rotor loop r1.*

The mutual inductance of bar #1 with respect to phases B and C can be readily found by analogy. Similarly, mutual inductances between the remaining bars and phases A, B, and C can be easily determined by analogy. Finally, when the number of stator phases is greater than three, the equations must be modified accordingly. However, again, the machine inductances are readily derived in a similar fashion.

2.7 Calculation of Inductances for the Induction Machine with one of the two coils in one phase disconnected

The specific machine studied in this paper to verify the theory is a three phase, 1 hp, 60 Hz, 4 pole, 208/460 V induction machine. The machine has 36 stator slots and 44 rotor bars. This machine has two coils per phase and the stator winding asymmetry is caused due to the disconnection of one of the coils in phase c. Figure 5 shows the turn function or the MMF distribution of the stator phases for the case of the balanced machine and for the case of stator winding asymmetry in phase c. Figure 6 shows the turn function distribution of the two adjacent rotor bars and the winding function of the rotor loop formed by the adjacent bars. The stator and rotor resistances and inductances are calculated as given in the Sections 2.3, 2.4 and 2.6. Table 1 gives the mutual inductances between the "healthy" phase a of the stator and rotor bar 1, as computed from the equations (36). Note that the mutual inductance between the phase b and rotor bar 1 is the same as given in Table 1 but shifted to the right by 6γ. Mutual inductance between phase a and rotor bar 2 is the same as given in Table 1, but shifted to the left by α. Table 2 gives

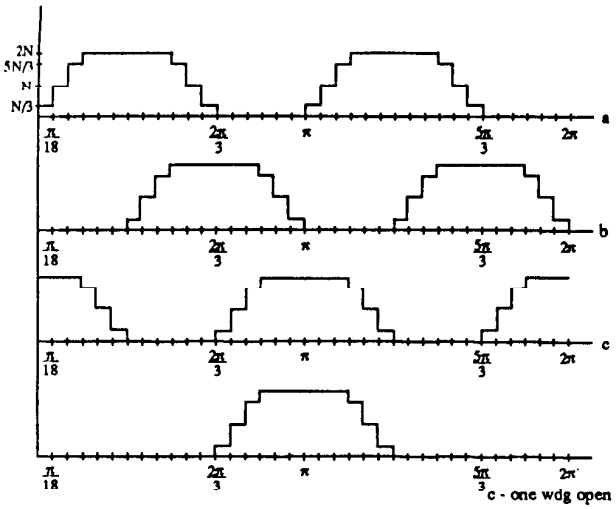

Figure 5: Turn Function of Stator Phases
(a): All phases "healthy'
(b): One coil in Phase C open

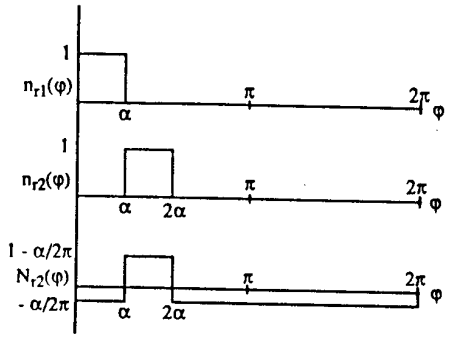

Figure 6: Turn Function of two adjacent Rotor Bars and winding function of one Rotor Bar

the mutual inductances between the shorted phase c of the stator and rotor bar 1. Figure 7 and Fig. 8 show the variation of the mutual inductance and incremental mutual inductance of the stator phases with one rotor bar, with respect to the rotor position.

For the case of the broken rotor bar, one rotor bar is considered broken and the resistances and the inductances are calculated as enumerated above.

As can be seen from the winding function diagrams of Figs. 5 - 8, the detailed modelling of the machine has been done considering each stator slots and each rotor bar and rotor loop, and no approximations such as the windings being concentrated under a pole face are done. For the specified applied stator voltages, the currents in each rotor loop, stator phase currents, stator and rotor fluxes, torque and speed are computed.

Table 1

$L_{A\,r1}$	Range of θ
$\frac{\mu_0 r l N}{g}\left[\frac{2\theta}{3} - \frac{\pi}{27}\right]$	$0 \le \theta < \frac{\pi}{9} - \alpha$
$\frac{\mu_0 r l N}{g}\left[\frac{4\theta}{3} + \frac{2\alpha}{3} - \frac{\pi}{9}\right]$	$\frac{\pi}{9} - \alpha \le \theta < \frac{\pi}{18}$
$\frac{\mu_0 r l N}{g}\left[\frac{2\theta}{3} + \frac{2\alpha}{3} - \frac{2\pi}{27}\right]$	$\frac{\pi}{18} \le \theta < \frac{\pi}{6} - \alpha$
$\frac{\mu_0 r l N}{g}\left[\theta + \alpha - \frac{7\pi}{54}\right]$	$\frac{\pi}{6} - \alpha \le \theta < \frac{\pi}{9}$
$\frac{\mu_0 r l N}{g}\left[\frac{\theta}{3} + \alpha - \frac{\pi}{18}\right]$	$\frac{\pi}{9} - \alpha \le \theta < \frac{\pi}{6}$
$\frac{\mu_0 r l N}{g}\alpha$	$\frac{\pi}{6} \le \theta < \frac{\pi}{2} - \alpha$
$\frac{\mu_0 r l N}{g}\left[-\frac{\theta}{3} + \frac{2}{3}\alpha + \frac{\pi}{6}\right]$	$\frac{\pi}{2} - \alpha \le \theta < \frac{5\pi}{9} - \alpha$
$\frac{\mu_0 r l N}{g}\left[-\theta + \frac{29\pi}{54}\right]$	$\frac{5\pi}{9} - \alpha \le \theta < \frac{\pi}{2}$

Table 2

$L_{C\,r2}$	Range of θ
$\frac{\mu_0 r l N}{g}\left[-\frac{\alpha}{2}\right]$	$0 \le \theta < \frac{2\pi}{3} - \alpha$
$\frac{\mu_0 r l N}{g}\left[\frac{\theta}{3} - \frac{\alpha}{6} - \frac{2\pi}{9}\right]$	$\frac{2\pi}{3} - \alpha \le \theta < \frac{13\pi}{18} - \alpha$
$\frac{\mu_0 r l N}{g}\left[\theta + \frac{\alpha}{2} - \frac{19\pi}{27}\right]$	$\frac{13\pi}{18} - \alpha \le \theta < \frac{2\pi}{3}$
$\frac{\mu_0 r l N}{g}\left[\frac{\theta}{2} + \frac{\alpha}{2} - \frac{10\pi}{27}\right]$	$\frac{2\pi}{3} \le \theta < \frac{7\pi}{9} - \alpha$
$\frac{\mu_0 r l N}{g}\left[\frac{4\theta}{3} + \frac{7\alpha}{6} - \pi\right]$	$\frac{7\pi}{9} - \alpha \le \theta < \frac{13\pi}{18}$
$\frac{\mu_0 r l N}{g}\left[\frac{2\theta}{3} + \frac{7\alpha}{6} - \frac{14\pi}{27}\right]$	$\frac{13\pi}{8} \le \theta < \frac{5\pi}{6} - \alpha$
$\frac{\mu_0 r l N}{g}\left[\theta + \frac{3\alpha}{2} - \frac{43\pi}{54}\right]$	$\frac{5\pi}{6} - \alpha \le \theta < \frac{7\pi}{9}$
$\frac{\mu_0 r l N}{g}\left[\frac{\theta}{3} + \frac{3\alpha}{2} - \frac{5\pi}{18}\right]$	$\frac{7\pi}{9} \le \theta < \frac{5\pi}{6}$
$\frac{\mu_0 r l N}{g}\left[\frac{3\alpha}{2}\right]$	$\frac{5\pi}{6} \le \theta < \frac{7\pi}{6} - \alpha$
$\frac{\mu_0 r l N}{g}\left[-\frac{\theta}{3} + \frac{7\alpha}{6} + \frac{7\pi}{18}\right]$	$\frac{7\pi}{6} - \alpha \le \theta < \frac{11\pi}{9} - \alpha$
$\frac{\mu_0 r l N}{g}\left[-\theta + \frac{\alpha}{2} + \frac{65\pi}{54}\right]$	$\frac{11\pi}{9} - \alpha \le \theta < \frac{7\pi}{6}$
$\frac{\mu_0 r l N}{g}\left[-\frac{2\theta}{3} + \frac{\alpha}{2} + \frac{22\pi}{27}\right]$	$\frac{7\pi}{6} \le \theta < \frac{23\pi}{18} - \alpha$

3. Simulation Results

The specification of the induction machine simulated are as given in Section 2.7. Simulation of the stator winding asymmetry due to the disconnection of one of the two coils of the phase c, and for the rotor asymmetry due to a broken rotor bar, are given for both the balanced sinusoidal voltage supply (208 V rms) and six-step voltage source inverter supply (V_{dc} = 269.7 V) . A no load operation has been assumed for all the cases.

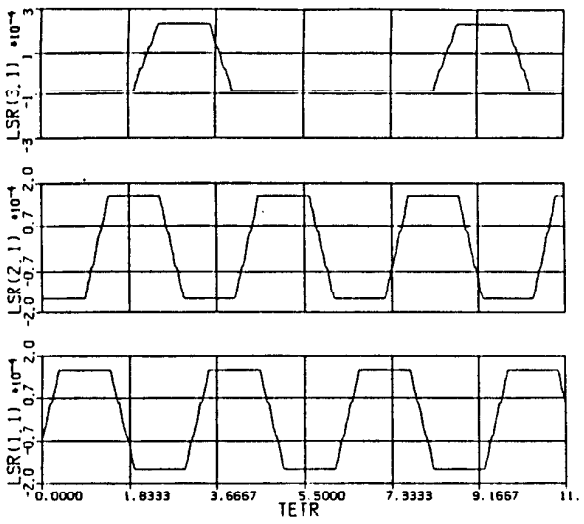

Figure 7: Mutual Inductances of Stator Phases a, b, and c (bottom to top) with Rotor Bar 1

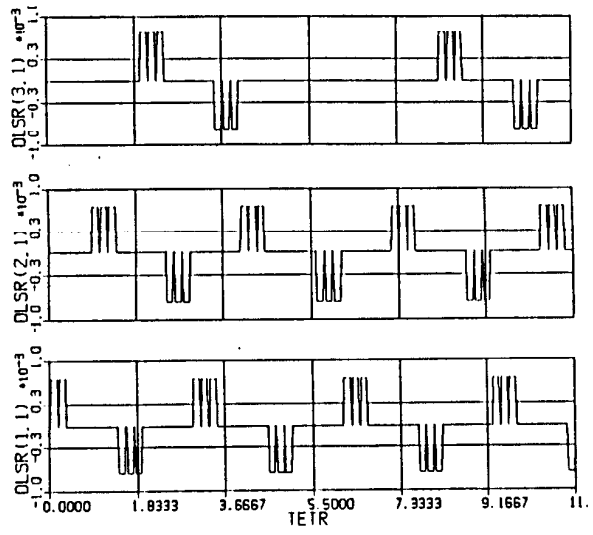

Figure 8: Incremental Mutual Inductances of Stator Phases a,b, and c (bottom to top) with Rotor Bar 1

Figure 9(a) shows the instantaneous electromagnetic torque, speed and the phase currents of the machine during a start up for the case of the balanced sinusoidal voltage supply. An increased current in the phase c of the machine is clearly seen, during transient and steady state conditions. This increase was noted to be approximately 40% compared to the symmetrically balanced case. Figures 9(b) and 9(c) show the steady state phase currents and the flux linkages of the machine under the same condition. The steady state phase c current is increased by approximately 40%, compared to the symmetrically balanced case. Figure 10 shows the instantaneous electromagnetic torque, speed and the phase currents of the machine during a start up for the case of machine supplied by a six-step voltage source inverter. In this case, also an increased current in the phase c of the machine during transient and steady state conditions is observed. The increase in the transient current in phase c, was noted to be approximately same as the case with stator asymmetry and balanced sinusoidal supply given in Fig. 9(a). However, the increase in the steady state current in phase c is observed to be approximately 10 -15% higher than the case with stator asymmetry and balanced sinusoidal supply given in Fig. 9(a). Further, the presence of large harmonics in the phase currents, as expected, is observed. The necessity for additional derating of the machine due to the inverter supply is evident.

Figure 11 shows the instantaneous electromagnetic torque, speed and the phase currents of the machine for the case of the a broken rotor bar, during a start up with a balanced sinusoidal voltage supply. It can be observed that the effect of a single broken bar on the machine phase currents in the transient and steady state is not very noticeable, as also stated in [21]. Hence, the detection of one broken rotor bar is not an easy task, but nevertheless, it is essential to be able to model the effect of broken rotor bars for accurate prediction of both the transient and steady state conditions,

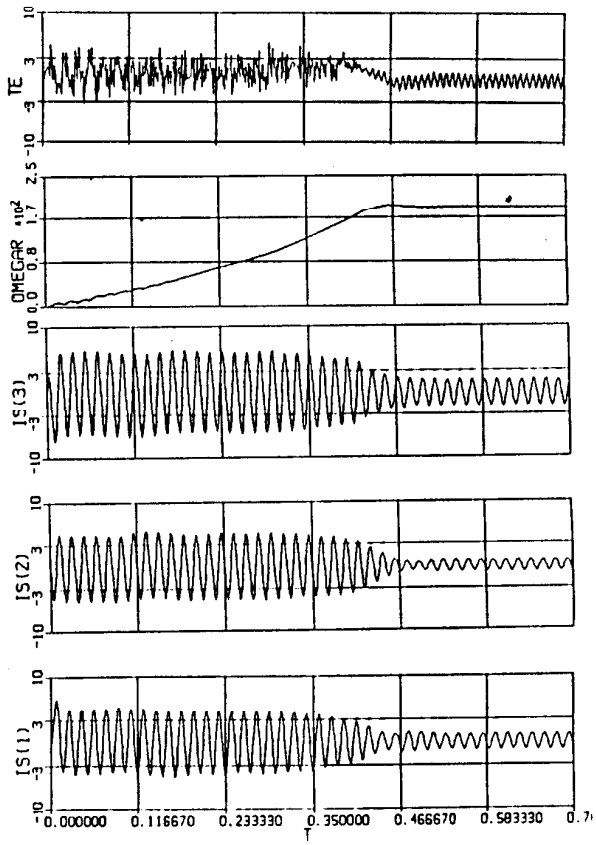

Figure 9(a): Stator Currents in phases a, b, and c; Speed; Torque (bottom to top) -- Sinusoidal Supply -- stator winding asymmetry

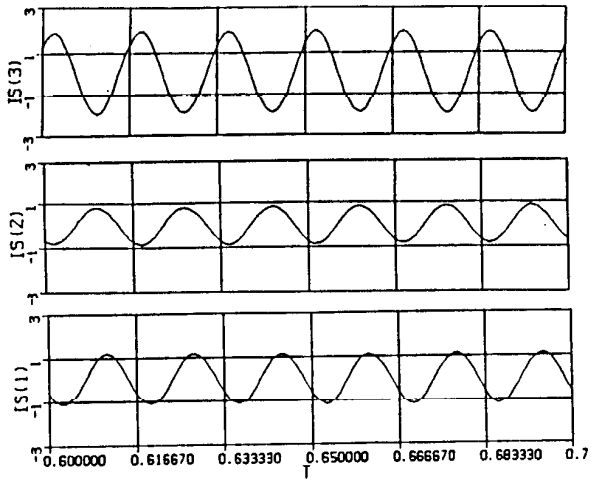

Figure 9(b): Steady State Stator Currents in phases a, b, and c (bottom to top) -- Sinusoidal Supply -- stator winding asymmetry

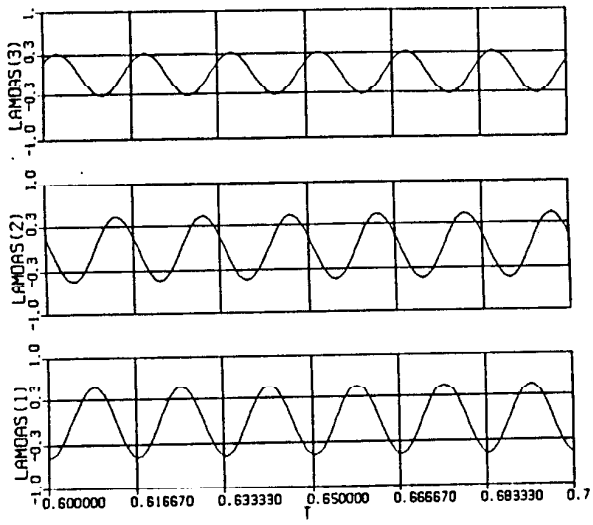

Figure 9(c): Steady State Stator Flux Linkages of Phases a, b, and c (bottom to top) -- Sinusoidal Supply stator winding asymmetry

for determination of torque degradation and rotor heating. The above method of winding function approach, can effectively model the induction machine with broken rotor bars for prediction of both the transient and steady state conditions.

Figures 12(a) and 12(b) show the instantaneous electromagnetic torque, speed and the phase currents of the machine, for the case of a broken rotor bar, supplied by a six-step voltage source inverter during start up transient and steady state respectively. It is interesting to note that a low frequency "beating" during the transient and steady state has been observed, as also mentioned in discussions of [15]. Further, the presence of large harmonics in the phase currents, as expected, is noticed.

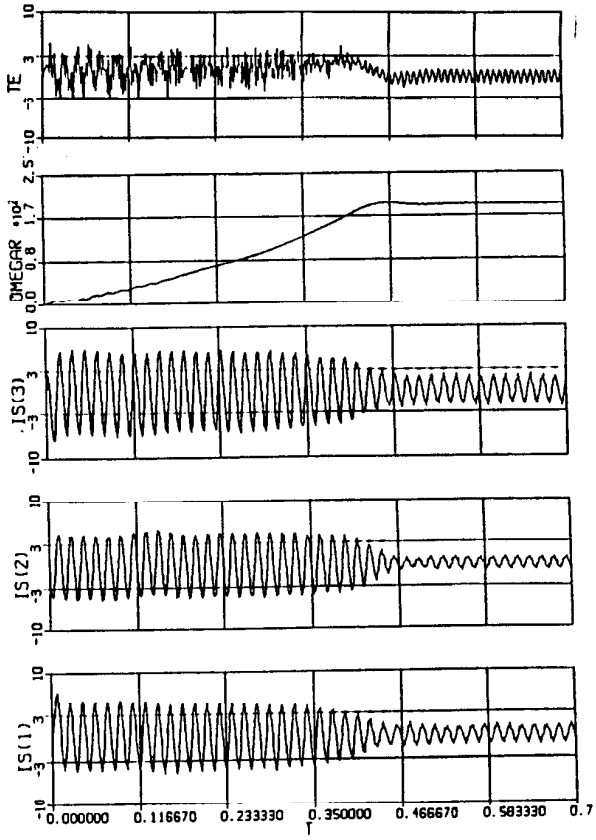

Figure 10: Stator Currents in phases a, b, and c; Speed; Torque (bottom to top) -- Six Step Inverter -- Stator winding asymmetry

Simulation results of Figs. 10, 12(a) and 12(b), emphasize the importance of this method in conjunction with inverter supplies for the determination of the peak instantaneous currents, required for the rating of the transistors.

It is important to note that the effects of space harmonics as simulated in this paper, typically result in torque pulsations. It should be mentioned that since the winding functions are modelled with sharp edges the effect of space harmonics are accentuated. Therefore, the higher frequency components observed in Figs. 10 and 12(a), would not be present in the real machine.

4. Experimental Results

Figure 13 shows experimental steady state phase currents for the above simulated induction machine with stator winding asymmetry due to the shorting of one of the two coils of the phase c, for the case of balanced sinusoidal voltage supply (208 V rms). As predicted by the simulation the phase c current is higher than the phase a

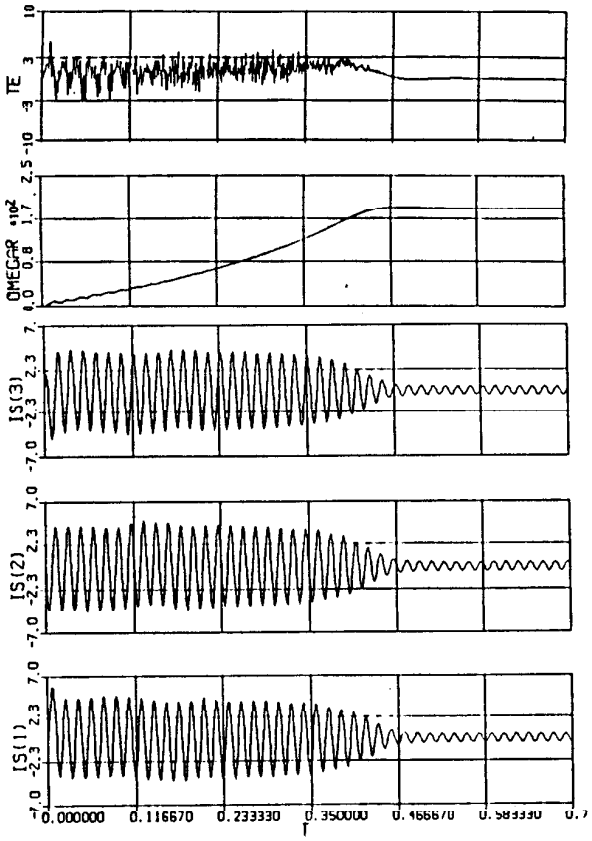

Figure 11: Stator Currents in phases a, b, and c; Speed; Torque (bottom to top) -- Sinusoidal Supply -- rotor winding asymmetry

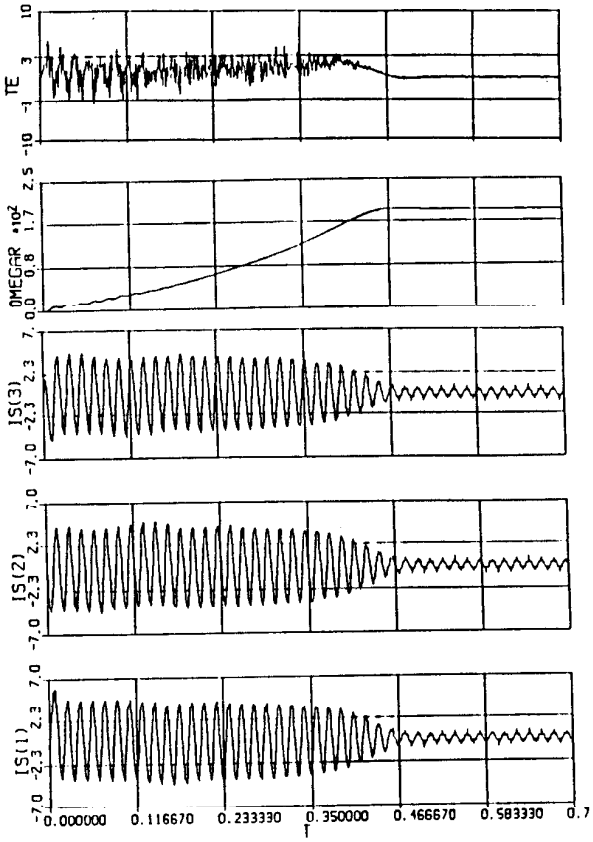

Figure 12(a): Stator Currents in phases a, b, and c; Speed; Torque (bottom to top) -- Six Step VSI -- rotor winding asymmetry

and b currents. The experimental results are in close agreement with the steady state simulation results given in Fig. 9(b).

Figure 14(a) shows experimental steady state phase currents for the above simulated induction machine with stator winding asymmetry due to the shorting of one of the two coils of the phases b and c, for the case of balanced sinusoidal voltage supply (208 V rms). In this case, as expected the phase b and c currents are large and 180 degrees with respect to each other and the phase a current is very much reduced. Also, it is interesting to note that a low frequency "beating" is observed in the phase currents in this case, as shown in Fig. 14(b).

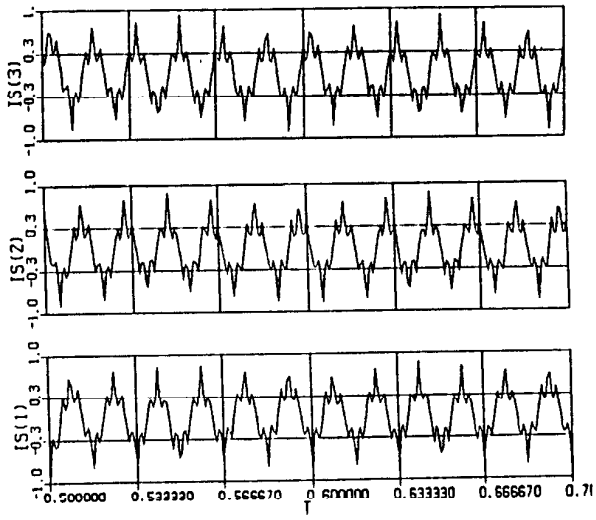

Figure 12(b): Steady State Stator Currents in phases a, b, and c (bottom to top) -- Six Step VSI -- rotor winding asymmetry

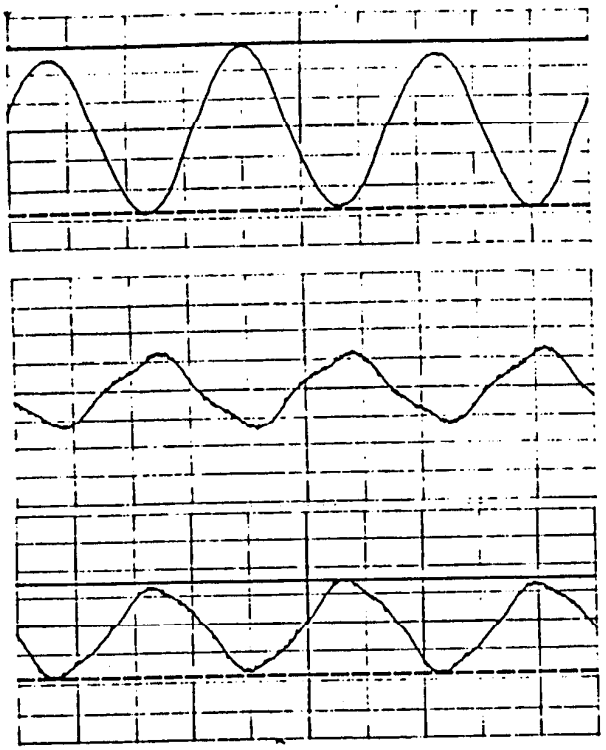

Figure 13: Experimental Results -- Steady State Stator Currents in Phases a, b, and c (top to bottom) -- Stator winding asymmetry in phase c -- Sinusoidal supply
Scale-- Current: 1A/div, Time: 5 ms/div

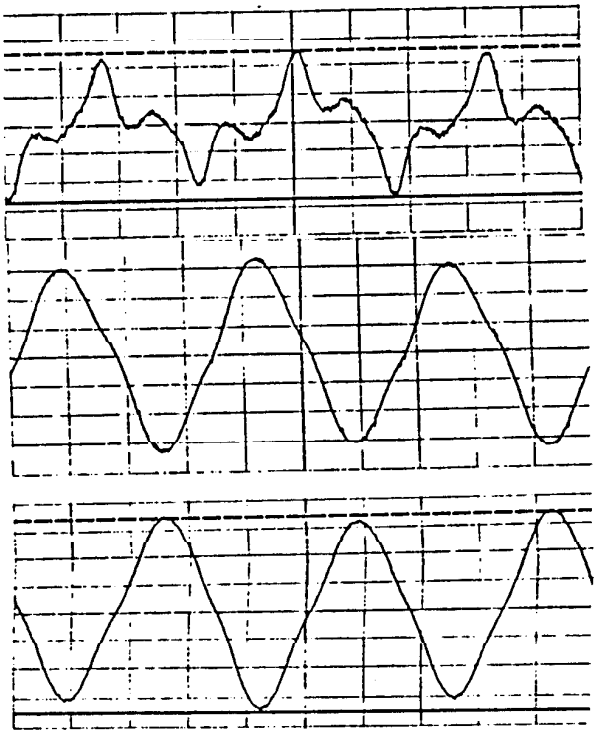

Figure 14(a): Experimental Results -- Steady State Stator Currents in Phases a, b, and c (top to bottom) -- Stator Winding asymmetry in phases b and c -- Sinusoidal supply. Scale: I_a : 50 mA/div I_b, I_c: 0.5 A/div; Time: 5 ms/div

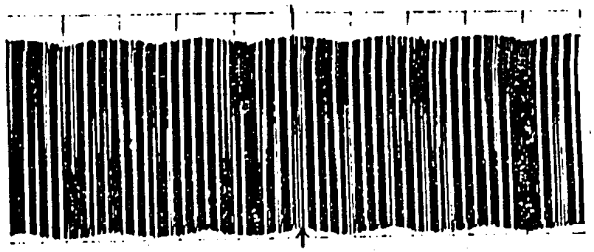

Figure 14(b): Low frequency "beating" in the current in Stator Phase c with stator winding asymmetry in phases b and c -- Balanced Sinusoidal Supply.
Scale: Current 0.5 A/div; Time: 1 s/div

5. Conclusion

The equations describing the performance of multiphase induction machines during the transient as well as steady state behavior including the computation of all machine inductances have been derived in this paper. In deriving these equations the space harmonics have been specifically included. Equations for calculation of electromagnetic torque have also been modified to account for non sinusoidal air gap flux distributions. Finally, to illustrate the utility of this method, a conventional 3 phase machine has been simulated, including the effects of space harmonics, for the case of stator asymmetry, and for the case of rotor asymmetry, with both balanced sinusoidal voltage supply and six-step voltage source inverter supply. Comparison of experimental and simulation results have verified the accuracy of the proposed method.

Acknowledgements

The authors wish to acknowledge the financial support provided by the Wisconsin Electric Machines and Power Electronics Consortium (WEMPEC) of the University of Wisconsin - Madison.

References:

[1] W.V. Lyon, C. Kingsley, "Analysis of unsymmetrical machines", AIEE Trans., Vol. 55, pp. 471-476, 1936.

[2] J.E. Brown, O.I. Butler, "A general method of analysis of 3-phase induction motors with asymmetrical primary connections", Proc. IEE, Vol. 100, Pt. II, pp. 25-34, 1953.

[3] J.E. Williams, "Operation of 3-phase induction motors on unbalanced voltages"; AIEE Trans., 73, Pt . III A, pp. 125-133, 1954.

[4] S.S. Murthy, B. Singh, A.K. Tandon, "Dynamic models for the transient analysis of induction machines with asymmetrical winding connections", Electric Machines and Electromechanics, Vol. 6, No. 6, pp. 479-492, 1981.

[5] S.S. Murthy, G.J. Berg, B. Singh, C.S. Jha, B.P. Singh, "Transient analysis of a three phase induction motor with a single phase supply", IEEE/PES Winter Meeting, 1982.

[6] J.E. Brown, C.S. Jha, "Generalised rotating field theory of polyphase induction motors and its relationship to symmetrical component theory", Proc. IEE, Vol. 109A, pp. 59-69, 1962.

[7] O.I. Butler, A.K. Wallace, "Generalised theory of induction motors with asymmetrical primary windings", Proc. IEE, Vol. 115, Pt. II, pp. 685-694, 1968.

[8] C.S. Jha, S.S. Murthy, "Generalised rotating field theory of wound-rotor induction machines having asymmetry in the stator and/or rotor windings", Proc. IEE, Vol. 120 (8), pp. 867-873, 1973.

[9] B.S. Guru, "Cross-field analysis of asymmetric three-phase induction motors - Extensions to single and two phase machines thereof", IEEE Trans. on PAS, Vol. 98, No. 4, July/Aug, 1979.

[10] A. Consoli, T.A. Lipo, "Orthogonal axis models for asymmetrically connected induction machines", IEEE Trans. on PAS, No.1, 1983.

[11] P. Vas, J.E. Brown, A. Shirley, "The application of N-phase generalized rotating field theory to induction machines with arbitrary stator winding connection", IEEE/PES Summer Meeting, 1983.

[12] F. Ciampolini, M. Martelli, C. Tassoni, "A new approach to dynamical analysis of asymmetrical induction motors supplied by non-sinusoidal voltage", 1985.

[13] T.A. Lipo, "The analysis of induction motors with voltage control by symmetrically triggered thyristors", IEEE Trans. on PAS, Vol. PAS-90, No.2, March/April 1971, pp. 515-525.

[14] S.S.Murthy, G.J. Berg, "A new approach to dynamic modeling and transient analysis of SCR-Controlled induction motors", IEEE/PES Winter Meeting, 1982.

[15] H.Weichel, "Squirrel-cage rotors with split resistance rings", Journal AIEE, 1928, 47, pp. 929-943.

[16] E. Mishkin, "Disturbances in the induction machine due to broken squirrel-cage rings", J. Franklin Inst., 1955, 259, pp. 133-143.

[17] P. Vas, "Investigation of squirrel cage induction motors with concentrated rotor asymmetries", Electrotechnika, Vol. 68, pp. 461-463, 1975.

[18] P. Vas, "Steady state operation of squirrel cage induction motors with general asymmetry", JEEE, (India), Vol. 59, pt. EL6, pp. 303-308, 1979.

[19] S. Williamson, A.C. Smith, "Steady-state analysis of 3-phase cage motors with rotor-bar and end-ring faults", Proc. IEE, 129, 1982, pp. 93-100.

[20] P.C. Krause, C.H. Thomas, "Simulation of symmetrical induction machinery", AIEE Trans. PAS, Vol. PAS-84, No. 11, Nov. 1965, pp. 1038-1053.

[21] G.B. Kliman, et. al., "Noninvasive detection of broken rotor bars in operating induction motors", IEEE Trans. on Energy Conversion, Vol. 3, No. 4, Dec. 1988, pp. 873-879.

[22] T.A. Lipo, "Theory and control of synchronous machines", ECE 511 Notes, University of Wisconsin-Madison, 1991.

[23] H.A. Toliyat, L. Xu, T.A. Lipo, "A five phase reluctance motor with high specific torque", IEEE/IAS Annual Meeting, 1990.

[24] H.A. Toliyat, T.A. Lipo, J.C. White, "Analysis of a concentrated winding induction machine for adjustable speed drive applications - Part 1 (Motor analysis)", IEEE/PES Winter Meeting 1990.

[25] H.A. Toliyat, T.A. Lipo, J.C. White, "Analysis of a concentrated winding induction machine for adjustable speed drive applications - Part 2 (Motor design and performance)", IEEE/PES Winter Meeting 1990.